



## ANALYSIS OF STRONG-MOTION ACCELEROGRAPH RECORDS OF THE 16 APRIL 2016 Mw 7.8 MUISNE, ECUADOR EARTHQUAKE

M. F. Gallegos<sup>(1)</sup> and G. R. Saragoni<sup>(2)</sup>

<sup>(1)</sup> MSc. Candidate, Department of Civil Engineering, University of Chile, e-mail: marco.gallegos@ug.uchile.cl ; mf.gallegos@engineer.com

<sup>(2)</sup> Professor, Structural Engineering-Division, Department of Civil Engineering, University of Chile, email: rsaragon@ing.uchile.cl

### Abstract

On April 16<sup>th</sup>, 2016, the Mw 7.8 Muisne earthquake ruptured a large area of the tectonic plate along Ecuador's pacific coast, causing several damages in many locations along the coast. The major city, near the epicentral area, was Pedernales with a maximum EMS-98 intensity reported of IX. Previous studies had shown that the northern coastal region, along the cities of Muisne and Pedernales (latitude 1°N to 0°, approximately), was coupled and remained unbroken since the January 1906 megathrust earthquake, suggesting the potential occurrence of a  $M > 7.5$  event the next decades. In addition, Carnegie Ridge enters the trench between 2.5°N and 1°S and its inferred subducted continuation is interpreted to be a "flat slab" configuration. With this background, Muisne earthquake hypocenter was located 20 km deep and its projection to surface was located over the continent. Hence, this event is one of the few subduction zone earthquakes well registered in terms of the closeness of the accelerographic stations to the seismic source.

A comprehensive analysis of the accelerograms for the 21 RENAC stations of the 2016 Muisne earthquake, originated by the subduction of the Nazca plate under the South American plate, is presented in this paper. The youth of the Nazca plate means that its surface has high density of asperities, which combined with its high convergence velocity, produces the highest seismicity zone of the world. Researchers had found Chile and Peru subduction accelerograms are characterized by high accelerations. For the Ecuadorian event, higher values of peak ground acceleration (PGA) and acceleration response spectra were observed. Moreover, the study of the destructiveness capacity of the accelerograms during this earthquake was performed by comparing their horizontal destructiveness potential factor (Pdh) with those calculated for the latest Chilean and Mexican seismic events.

Two-peak response spectra were previously observed in some stations of Chilean interplate thrust earthquakes in 1985 and 2010. When the accelerations are recorded at the epicentral zone stations, the response spectra are more complex, having two peaks in some cases. Similar response spectra with two predominant peaks were observed for Pedernales station, which was located 36 km SW of the epicenter. Furthermore, free soil vibrations were detected at Chone station analyzing the spectrogram of its acceleration record. Finally, the period of the second peak in the response spectra of these two representative stations of the 2016 Muisne earthquake agrees approximately with the soil deposit natural period determined by the Nakamura's H/V spectral ratio from their accelerogram codas.

The Muisne earthquake shows greater PGA and Pdh values than other important subduction earthquakes, like 1985 Mw 7.8 Valparaiso - Chile, 1985 Mw 8.1 Michoacán - Mexico and 2010 Mw 8.8 El Maule – Chile. In addition, soil effects could be inferred due to the high destructiveness potential, the low zero crossing intensity and free soil vibration phenomenon in some accelerograms. All these remarks evidence the high seismic hazard in Ecuador and represents a warning voice for the future development of high-rise building projects in many cities settled over soft soils along the country.

**Keywords:** Ecuador's subduction earthquake; Accelerogram; Destructiveness potential; Two-peak response spectra; Soil effect.



## 1. Introduction

Ecuador is located in the Pacific Ring of Fire, shared by almost all continental and insular coasts bathed by the Pacific Ocean, within which about 90% of the world's earthquake energy release. Offshore its coasts, the Nazca plate is subducting eastwards beneath the South America plate at a rate varying from approximately 55 to 58 mm per year. Further, the coastline is on average less than 75 km from the trench axis [1]. Hence, Ecuador has a long history of large earthquakes, as the result of shallow thrust faulting near the plates boundary.

During 1906, three  $M > 8$  earthquakes occurred along the Pacific coast of America (San Francisco, USA; Valparaiso, Chile; and Esmeraldas, Ecuador) causing large damages and several deaths. The Mw 8.8 Esmeraldas-Tumaco megathrust earthquake, offshore of the Ecuadorian and Colombian coast, is the seventh largest in magnitude seismic event in the world [2]. Chronicles of that time [3] reported huge macroseismic intensities due to large ground motions for long five minutes and a damaging tsunami that caused in the region of 500-1.500 fatalities. This 1906 event shares many similarities with the 2010 Mw 8.8 El Maule, Chile earthquake that was also a bi-lateral rupture with a total length of about 550 km. In the last century, at least four more  $M > 7$  subduction earthquakes ruptured the plate along the Ecuadorian margin. Table 1 shows some characteristics of these historic interplate thrust seismic events [4 - 8].

Table 1 – Ecuadorian subduction seismic events in the 20th century.

Date	Magnitude	Latitude	Longitude	Depth [km]	Rupture Length [km]
1906	8.8	1.00 <sup>0</sup> N	81.50 <sup>0</sup> W	-	500
1942	7.8	0.01 <sup>0</sup> N	79.90 <sup>0</sup> W	35	200
1958	7.7	0.99 <sup>0</sup> N	79.49 <sup>0</sup> W	19	50
1979	8.1	1.60 <sup>0</sup> N	79.36 <sup>0</sup> W	24	240
1998	7.2	0.60 <sup>0</sup> S	80.31 <sup>0</sup> W	26	-

Ecuador has a complex seismotectonic setting with the subduction of the oceanic Nazca plate and South America Craton. Nocquet et al. [9], based on GPS measurements, proposed that the continental deformation partitioning is highly controlled by the diverging motion of two continental slivers: the Inca Sliver and the North Andean Sliver. Fig. 1-a shows this seismotectonic setting. The black color ellipse indicates the approximate rupture of the great 1906 megathrust earthquake.

The Interseismic Coupling (ISC) is used as a qualitative measure of the mechanical interaction between two converging tectonic plates between two large earthquakes, with a heterogeneous pattern of highly coupled patches separated by creeping patches that is consistent with the concept of the asperity model. Chlieh et al. [10] studied in detail the interseismic coupling in north coast of Ecuador, selecting the 30 GPS sites located between the trench and the eastern boundary of the North Andean Sliver. Thus, a discrete asperity distribution along the interplate contact was proposed, indicating that the coupling was weak and very shallow in south Ecuador and increases northward. The models indicated three large asperities. First one in southern Ecuador that extends from Santa Elena Peninsula to Island of La Plata. Second one in Central Ecuador from Bahía de Caráquez to the Atacames promontory, where 1942 and 1998 earthquakes were located. Finally, a third asperity from Esmeraldas to Manglares where 1958 and 1979 earthquakes were located. The great 1906 rupture probably involved the failure of the two very large (or five smaller) asperities found between 0.5°S and 2°N, i.e., the Bahía de Caráquez–Atacames and the Esmeraldas–Manglares asperities. Fig. 1-b indicates this asperity distribution.

With this background, at 23:58:36 (UTC) of the 16 April 2016, an Mw 7.8 earthquake occurred as the result of shallow thrust faulting near the plates boundary in the Ecuadorian northern coastal region. The epicenter was located at 0.4°N, 79.9°W, near the cities of Muisne and Pedernales, and a depth of 20 km [11]. The event confirms the concept of the seismic gap, completing the seismic cycle that began in 1906. This event

is placed at the southern end of the approximate rupture area of the 1906 event and probably has similar rupture area and magnitude of the 1942 event. In Fig. 1-b, the red color star indicates the epicenter and the rupture area, limited by the locations of aftershocks, are drawn as red color rectangle for the 2016 Muisne earthquake.

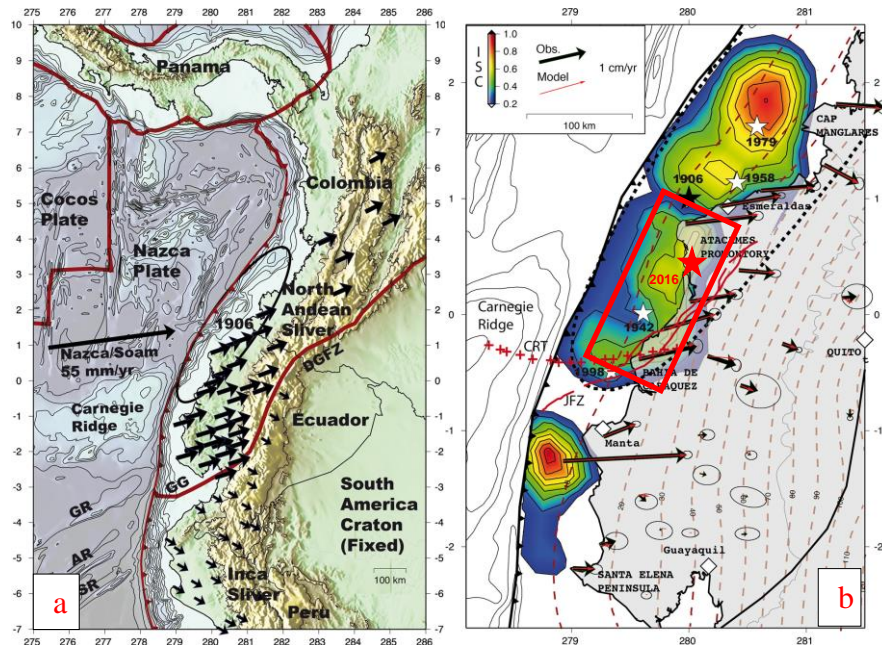


Fig. 1 – a) Seismotectonic setting of Ecuador: Nazca, South America plates and Inca, North Andean slivers.  
 b) Interseismic coupling showing the main asperities and location of the 2016 Muisne earthquake (modified from Chlieh et al. [10]).

The innovations in Earthquake Engineering over the past 50 years, have provided powerful tools to estimate and to reduce building destruction, and consequently losses of lives. The seismic hazard or the potential ground shaking of an area produced by earthquakes can be estimated from the local seismotectonics and records of strong-motions accelerographs [12]. The analysis of the accelerograms allows to characterize the most relevant aspects of these earthquakes, and their effects on any type of structures. The April 2016 Muisne earthquake was the largest earthquake in terms of acceleration recorded by the National Accelerometer Network (RENAC) of the Instituto Geofísico at the Escuela Politécnica Nacional (IG-EPN) [13].

In this paper, a comprehensive analysis of the accelerograms for the 21 RENAC stations of the 2016 Muisne earthquake is performed, obtaining some characteristics such as maximum horizontal and vertical acceleration, Arias intensity and destructiveness potential. These values show a quantitative measure that can be related to the European macroseismic scale of intensities, to identify the level of damage in the affected area. Then, acceleration spectra of Pedernales and Chone stations are obtained due to their quantities are related to the maximum values in terms of acceleration and destructive potential. Before, these stations are compared with those from some Chilean subduction seismic events such as 1985 Valparaíso and 2010 El Maule. In addition, a study of free soil vibrations using an analysis time to frequency is performed, which allows to identify the energy release in time, as also the site effect from the response spectra. Further, the H/V spectral ratio for the horizontal and vertical acceleration components was obtained by Nakamura method, resulting possible to obtain the fundamental frequency of the soil deposit.

Finally, these analyzes confirm the importance of Ecuador from a geographic point of view in the contribution to the seismic characterization of subduction events for the interaction between Nazca and South American plates. Additionally, these remarks show a capacity to generate the maximum events seismic data to the date recorded, not only in terms of acceleration but also in other damage measures. The study of the seismic hazard is one the keys in the identification of the risk hazard, being fundamental to mitigate the seismic vulnerability in Latin America.

## 2. Accelerographic Data

Muisne earthquake hypocenter was located 20 km deep and its projection to surface was located over the continent. Hence, this event is one of the few subduction zone earthquakes well registered in terms of the closeness of the accelerographic stations to the seismic source (36 km SW from the epicenter).

IG-EPN recovered information from 21 accelerographic stations with strong-motion instruments deployed across the country [13]. Fig. 2 shows the same scale accelerograms in the EW direction for the 13 major cities. In this figure, the red color accelerogram corresponds to Pedernales station (APED), where the greatest peak ground acceleration of  $13.805 \text{ m/s}^2$  or 1.41 g. was recorded. Green color rectangle indicates the rupture area of  $160 \text{ km} \times 60 \text{ km}$  [11] and aftershocks of magnitude  $M > 6.0$  are drawn as purple color circles [14].

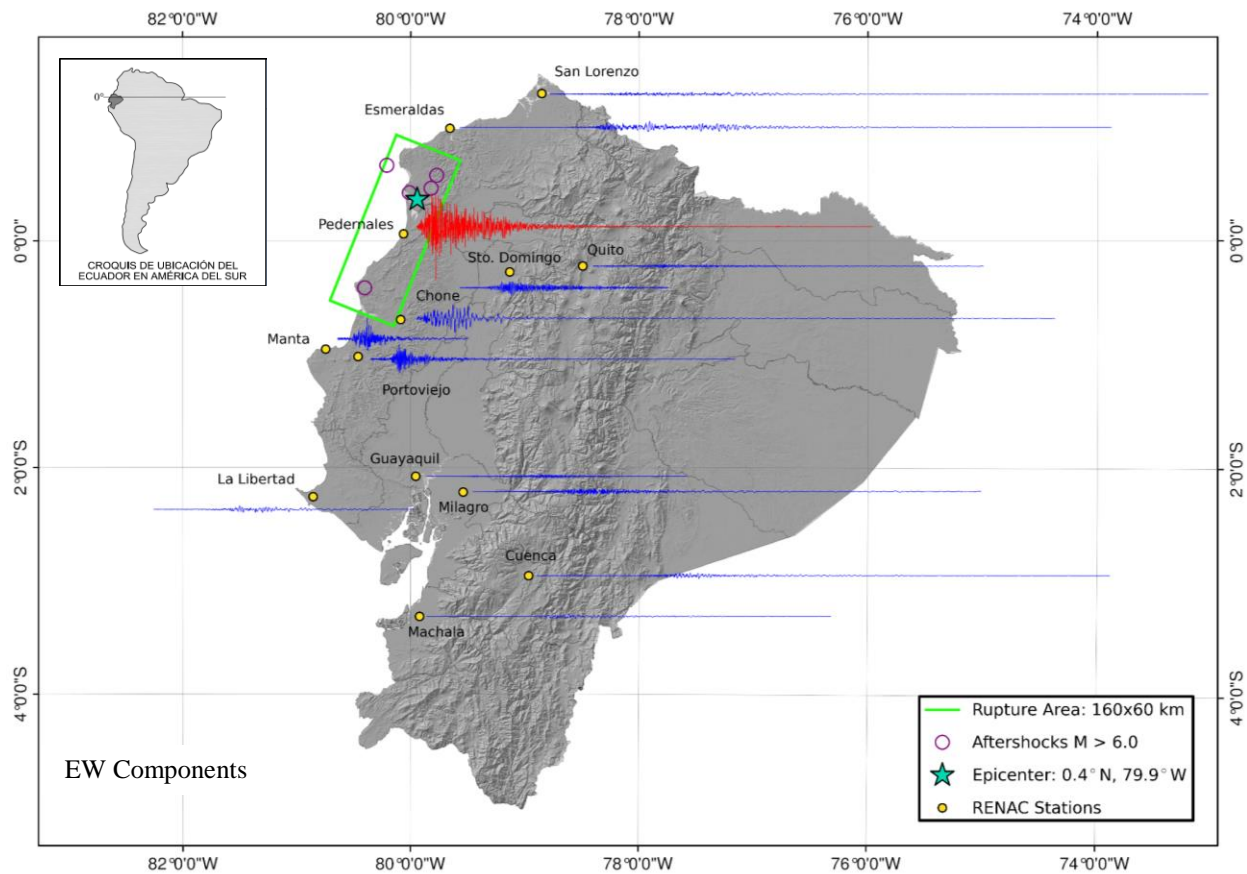


Fig. 2 – Accelerographic EW components for 2016 Muisne, Ecuador earthquake.

Fig. 2 furthermore shows significant differences between the waveforms and duration of some accelerograms. The duration of the earthquake lasted between 60 to 120 seconds approximately. Phenomena like attenuation, directivity and amplification, which are typical of subduction seismic events in Chile and Peru with elongated elliptic shape of the shaken area in a direction parallel to the coastline, is also observed in the Muisne earthquake. Isoseismal maps for some subduction earthquakes in South America are shown in Fig. 3.

The Andean Mountains act as a natural barrier, providing greater seismic attenuation in the EW direction due to the wave reflections and refractions in the multiple geological interfaces. For stations located at the mountains, like Quito and Cuenca with epicentral distance larger than 200 km, lower accelerations were detected in comparison to coastal stations.

Rupture direction is another important issue. At north (Esmeraldas and San Lorenzo stations), the peak acceleration values were lower, but the duration was longer. While at south (Portoviejo, Manta and Chone

stations), greater peak accelerations were obtained with a shorter duration. This result confirms that the fault rupture direction was NS.

Large damages in downtown of Portoviejo, Manta and Chone cities were reported by many reconnaissance teams after the earthquake [15]. Accelerograms show stronger ground motions for these stations. Dynamic amplification phenomenon by local site conditions, such as soft soil, could be inferred due to collapses of some reinforced concrete frame and masonry buildings.

Plate roughness, which is linked to plate age, is a key factor in the frequency content of earthquake accelerograms and is always related with peak ground acceleration. Maximum acceleration is important in seismic risk studies due to the damage capacity of earthquakes is arbitrary associated to the probability of exceedance of horizontal PGA.

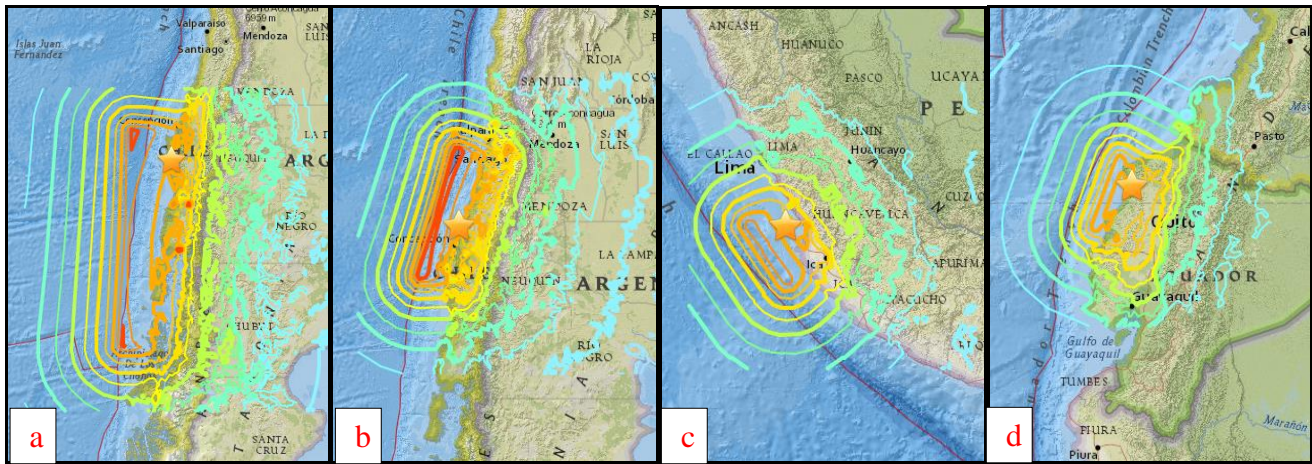


Fig. 3 – Isoseismal maps for subduction interplate earthquakes in South America (figures from USGS).

- a) 1960 Mw 9.5 Valdivia, Chile. b) 2010 Mw 8.8 El Maule, Chile.
- c) 2007 Mw 7.9 Pisco, Peru. d) 2016 Mw 7.8 Muisne, Ecuador.

Table 2 shows the characteristics of the accelerograms for 21 RENAC accelerographic stations, indicating their peak ground acceleration (PGA) in units of acceleration of gravity, zero crossing intensity ( $v_0$ ), Intensity of Arias (Ia), Destructiveness potential factor (Pd), Horizontal destructive potential (Pdh) and European Macroseismic Scale intensity (EMS-98) estimated by IG-EPN. Stations are ordered from highest to lowest horizontal destructiveness potential Pdh.

Maximum macroseismic intensity during this earthquake was reported for the city of Pedernales (APED). The station accelerogram has the maximum horizontal acceleration with 1.41 g. for EW component. This maximum acceleration value is larger than value recorded for the 2010 Mw 8.8 El Maule earthquake, Cauquenes station with 1.25 g. Moreover, it corresponds to more than twice the value recorded for the 1985 Mw 7.8 Valparaiso earthquake, Llolleo station with 0.67 g. [16]. It is important to note that Valparaiso seismic event had similar moment magnitude than 2016 Muisne earthquake.

In addition, Pedernales has the maximum vertical acceleration with 0.74 g. This high vertical acceleration value close to 1 g. is associated with coastal rise phenomenon, a characteristic of the subduction seismotectonics noticed previously in Chilean earthquakes. Southern stations: Manta (AMNT), Portoviejo (APO1) and Chone (ACHN), have high values of PGA, especially for NS direction with 0.52, 0.38 and 0.37 g., respectively. These facts ratify that the fault rupture was NS direction.

On the other hand, more than a half of the stations exhibited accelerations lower than 0.05 g. for both components. One of the most important limitations for a comprehensive interpretation of acceleration records is the nonexistent soil dynamic classification for most of stations. Fig. 4 shows the horizontal and vertical components of accelerograms for Pedernales and Chone stations measured as percentage of gravity.

Table 2 – Accelerogram characteristics of the 2016 Muisne earthquake. EMS-98 intensities (by IG-EPN), Peak ground acceleration (PGA), Intensity of Arias (Ia), zero crossing intensity ( $v_o$ ), Destructiveness potential (Pd) and Horizontal destructiveness potential (Pdh).

Nº	STAT.	CITY	DIR.	EMS-98 IG-EPN	Ep. Dist. km	PGA g	Ia g-sec	$v_o$ z-cr/sec	Pd cm-sec	Pdh cm-sec
1	ACHN	CHONE	E-W N-S Z	7	120	0.33 0.37 0.17	0.51 0.53 0.07	1 1 3	259.29 324.22 8.43	583.51
2	APED	PEDERNALES	E-W N-S Z	9	36	1.41 0.83 0.74	2.95 1.94 0.66	5 6 10	110.46 48.90 6.82	159.36
3	AES2	ESMERALDAS	E-W N-S Z	5	76	0.15 0.11 0.04	0.18 0.11 0.02	2 2 8	35.57 22.04 0.41	57.61
4	APO1	PORTOVIEJO	E-W N-S Z	7	167	0.32 0.38 0.10	0.28 0.33 0.03	3 3 3	23.16 26.55 3.19	49.71
5	AMNT	MANTA	E-W N-S Z	7	171	0.40 0.52 0.17	0.26 0.23 0.04	7 6 8	4.88 7.52 0.69	12.40
6	ASDO	SANTO DOMINGO	E-W N-S Z	5	115	0.21 0.11 0.05	0.17 0.06 0.01	5 6 10	5.71 2.09 0.13	7.80
7	AIB1	IBARRA	E-W N-S Z	4	202	0.05 0.06 0.01	0.02 0.02 0.002	3 3 4	2.23 1.72 0.11	3.95
8	ALOR	SAN LORENZO	E-W N-S Z	4	159	0.03 0.03 0.02	0.01 0.01 0.003	2 1 3	1.69 1.76 0.37	3.45
9	ALIB	LA LIBERTAD	E-W N-S Z	5	308	0.04 0.04 0.02	0.01 0.01 0.002	2 2 2	1.48 1.69 0.57	3.17
10	AMIL	MILAGRO	E-W N-S Z	5	288	0.05 0.05 0.02	0.01 0.01 0.002	3 3 4	1.24 1.19 0.12	2.43
11	ACUE	CUENCA	E-W N-S Z	4	381	0.04 0.03 0.02	0.01 0.01 0.003	3 2 3	0.94 1.12 0.43	2.06
12	ACH1	MACHALA	E-W N-S Z	4	407	0.03 0.02 0.01	0.004 0.01 0.001	3 2 3	0.68 1.02 0.07	1.70
13	AOTA	OTAVALO	E-W N-S Z	4	188	0.04 0.04 0.02	0.01 0.01 0.003	4 4 5	0.79 0.65 0.11	1.44
14	AIB2	IBARRA - 2	E-W N-S Z	4	204	0.02 0.03 0.01	0.004 0.01 0.001	3 3 4	0.38 0.71 0.05	1.09
15	ATUL	TULCÁN	E-W N-S Z	4	251	0.02 0.02 0.01	0.003 0.003 0.0005	3 3 3	0.38 0.40 0.05	0.78
16	PRAM	QUITO	E-W N-S Z	4	171	0.03 0.02 0.01	0.005 0.01 0.002	4 3 5	0.27 0.48 0.08	0.75
17	AAM2	AMBATO	E-W N-S Z	4	235	0.03 0.04 0.02	0.01 0.01 0.002	5 4 5	0.24 0.45 0.10	0.69
18	ALAT	LATACUNGA	E-W N-S Z	4	206	0.03 0.03 0.01	0.01 0.01 0.001	4 4 4	0.33 0.35 0.08	0.68
19	EPNL	QUITO - EPN	E-W N-S Z	4	174	0.03 0.02 0.01	0.004 0.004 0.002	4 4 4	0.29 0.34 0.12	0.63
20	ALJ1	LOJA	E-W N-S Z	4	492	0.02 0.02 0.01	0.001 0.001 0.001	3 3 3	0.20 0.20 0.05	0.40
21	AGYE	GUAYAQUIL	E-W N-S Z	6	270	0.02 0.02 0.02	0.001 0.002 0.001	17 17 17	0.004 0.005 0.003	0.01

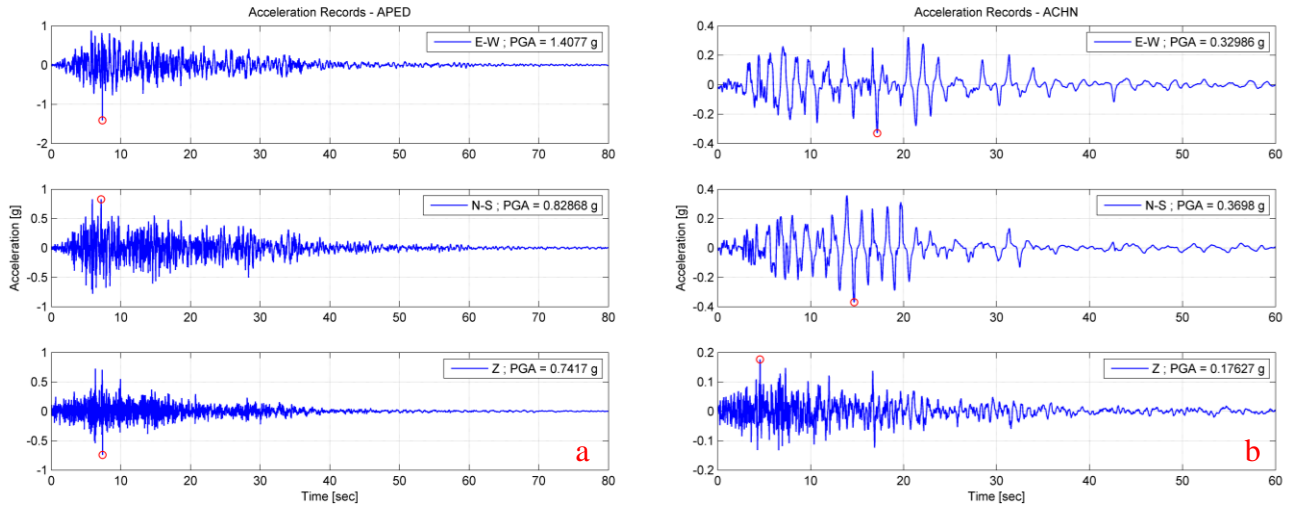


Fig. 4 – Horizontal and vertical component accelerograms, 2016 Muisne, Ecuador earthquake.  
a) Pedernales station (APED). b) Chone station (ACHN).

### 3. Arias Intensity

The Arias intensity ( $I_a$ ) is a parameter that reflects the total energy contained in an accelerogram and is related to the capacity of the ground seismic motions to produce damage in structures. This parameter represents the sum of energy dissipated per unit mass by a set of one-degree-of-freedom damped elastic oscillators, whose frequencies are uniformly distributed throughout the frequency range between 0 and infinity [17]. The instrumental intensity, defined according Eq. (1), was computed for horizontal and vertical components for all stations and is presented in Table 2. Pedernales station shows the largest values with 2.95 g-sec and 1.94 g-sec for EW and NS directions, respectively.

$$I_a = \frac{\pi}{2 * g} \int_{t_0}^{t_0+D} a_g(t)^2 dt \quad (1)$$

Where  $I_a$  is the Arias Intensity,  $g$  is the acceleration of gravity,  $t_0$  and  $D$  corresponds to initial time and duration of the accelerogram, and  $a_g(t)$  is the acceleration record.

### 4. Destructiveness Potential Factor

The destructiveness potential factor ( $P_d$ ), defined by Araya and Saragoni [18], is an instrumental intensity based on the strong nonlinear earthquake response of one-degree-of-freedom elastoplastic structures. Due to the intensity of zero crossings plays an important role in the earthquake destructiveness, this parameter relates the capacity of earthquake ground motion to produce structural and soil damage and the intensity of zero crossings per second of the acceleration record.  $P_d$  expressed in terms of Arias intensity is shown in Eq. (2), where  $v_o$  corresponds to intensity of zero crossings per second.

$$P_d = \frac{I_a}{v_o^2} \quad (2)$$

$P_d$  is proportional to the average ductility spectrum of simple elastoplastic nonlinear oscillators of one degree of freedom. In addition, the horizontal destructiveness potential factor ( $P_{dh}$ ) includes the simultaneous effect of orthogonal horizontal accelerogram components, resulting in Eq. (3).

$$P_{dh} = P_{dx} + P_{dy} \quad (3)$$



Several studies and research have shown that destructiveness potential factor is quite well correlated with the observed damages and with the equivalent macroseismic intensities. This is the most complete parameter and the one that best adjusts to the observed damages. Saragoni et al. [19], studied more than 300 accelerograms of world earthquakes and defined destructive accelerograms which satisfied their Pdh larger than 4.0 cm-sec, corresponding to VII in the Modified Mercalli intensity scale (MMI). Saragoni et al. [20] evaluated the destructiveness of subduction Chilean and Peruvian earthquakes during the last 60 years. It was found that 1985 M 7.8 Valparaiso earthquake (Llolleo station) and 2007 M 7.9 Pisco earthquake (Ica2 station) had the greatest Pdh values with 27.6 and 22.4 cm-sec, respectively. Later, Saragoni and Ruiz [16] obtained the maximum value Pdh of 110.9 cm-sec at Constitución station for the 2010 El Maule earthquake, which corresponds to the maximum value registered in Chile. Finally, Saragoni and Herrera [21] discovered higher Pdh values for the 1985 Mw 8.1 Michoacán earthquake with 321.8 and 193.4 cm-sec for Tlahuac Bombas and STC stations in Mexico City (associated with the collapse of many tall buildings, 7 to 15 floors), respectively. Nevertheless, 2016 Muisne earthquake have surprises larger values. Table 2 shows the highest Pdh value in the world of 583.5 cm-sec at Chone station related to a low intensity of zero crossing per second of 1. Meanwhile, Pedernales station has the second Pdh value of 159.4 cm-sec for this event, where the maximum macroseismic intensity of IX was recorded.

Table 2 furthermore shows several stations have destructive accelerograms. These stations correspond to six cities where damaging conditions and building collapses were observed by reconnaissance teams in the northern coastal region of the country. From stations N° 7 Ibarra-1 to N° 20 Loja the accelerograms are not destructive. Despite Guayaquil station has the lowest Pdh value, macroseismic intensity of VI (strong) was reported for the city. This fact is due to the station is located over superficial rock, while downtown is settled over soft silt/sandy soils. More specific studies about soil effect analyzing some accelerograph records deployed across the city of Guayaquil have been performed by Laurendeau et al. [22].

Many non-technical causes were found by experts to explain the bad seismic performance of most concrete and masonry buildings, such as self-construction, soft first story, short columns, poor steel reinforcement details and corrosion, etc. [15]. Despite this reality, the instrumental analysis of both values: PGA and Pdh, confirms the observations indicating that the Muisne earthquake was destructive. This remark agrees with the observed behavior especially of structures of low and medium height in the cities located near the epicentral area. However, high Pdh values calculated for Chone and Pedernales stations suggest their accelerograms are very destructive, especially for high-rise buildings that for the day of the earthquake still did not exist in these cities.

## 5. Two-Peak Response Spectra of Pedernales station

Absolute acceleration response spectra, for 5% critical damping, for the 21 RENAC stations were computed. Analyzing the spectra corresponding to the horizontal components, Pedernales and Chone stations exhibit a remarkable behavior. The first one, the nearest station to the epicenter, is characterized to have their spectra with two predominant peaks. One of them between 0.5 and 0.6 sec., which would belong to the free vibrations of the soft soil; and another peak around 0.1 sec., due to probably the interaction of the waves associated with the seismic source and the response of higher ground modes (2nd and 3rd vibration modes). Two-peak response spectra were previously observed in some Chilean interplate thrust earthquakes. Saragoni and Ruiz [16] concluded that when the soil response is deterministically dominated in most accelerograms, response spectra are characterized to have a single peak, as indicated by most seismic design codes. However, when the accelerations are recorded at the epicentral zone stations, the response spectra are more complex, having two peaks in some cases.

In Fig. 5, acceleration response spectra of two peaks, corresponding to EW and NS directions of some South America interplate subduction earthquakes for epicentral stations, are plotted. In these figures, the green color spectra corresponding to 2016 Muisne earthquake (Pedernales station) is compared with those spectra from 2010 El Maule earthquake (Concepcion station) and 1985 Valparaiso earthquake (Viña del Mar station); in blue and red color spectra, respectively. From the comparison of the spectra, two predominant peaks are clearly seen

in all acceleration spectra for both components. It is important to note that peak 1 and peak 2 for each seismic spectrum has similar acceleration amplitude. Moreover, the highest values of absolute acceleration response spectra occur for the Ecuadorian earthquake with maximum values close to 3.5 g. Finally, the periods where first and second peaks of the spectra are different for each city, related possibly with soil type, rupture direction or magnitude. Despite this observation, the ratio between periods  $T_2$  and  $T_1$  is almost similar for three spectra around values of 3 to 4.

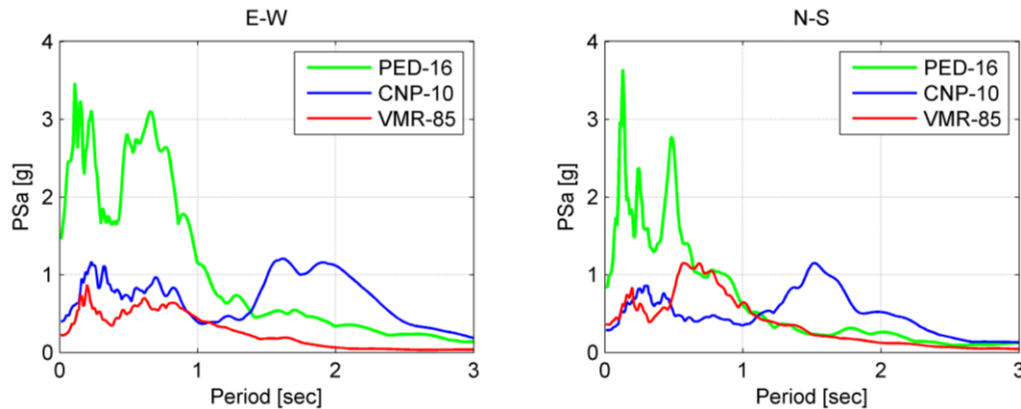


Fig. 5 – Two-peak acceleration response spectra for South America interplate subduction earthquakes,  $\beta=5\%$ . Green: Pedernales station, 2016. Blue: Concepción station, Chile 2010. Red: Viña del Mar station, Chile 1985.

## 6. Free Soil Vibrations in Chone station Accelerogram

In accelerograms of large earthquakes it is common to observe free vibrations of the soil [23]. This is due to the energy released of the seismic sources, especially of their asperities, does not arrive permanently, leaving intervals in which no seismic waves arrived, developing free soil vibrations. A spectrogram is a visual representation of the spectrum of frequencies in a seismic record as they vary with time. Saragoni and Ruiz [16] observed this kind of vibrations for 2010 Mw 8.8 El Maule earthquake through the spectrogram of Concepcion station. They saw the intervals where the soil responded freely at a frequency of 0.5 Hz. between energy arrivals. Fig. 6-up shows the Chone station accelerogram for NS direction where free soil harmonic vibrations between 5 to 35 sec. of the total record duration are observed. In the spectrogram of Fig. 6-down the intervals where the soil responded freely at a frequency of 0.6 to 0.7 Hz., between the arrivals of energy corresponding to higher frequencies, are clearly seen.

Saragoni and Ruiz [16] also found for 2010 event, that accelerograph records had a dual character, in which the accelerograms recorded away from the rupture area are characterized due to free vibrations exceed seismic waves, whereas the seismic source waves are predominant for epicentral acceleration records. These observations are confirmed for the 2016 Muisne earthquake.

In Fig. 7, absolute acceleration response spectra, for 5% critical damping, corresponding to EW and NS directions of two subduction earthquakes far away of epicentral zone, are plotted. In these figures, the green color spectra corresponding to 2016 Muisne earthquake (Chone station) is compared with the spectra from 1985 Michoacán earthquake (SCT, Mexico City station) in blue color. From the comparison of the response spectra, both stations exhibit a main peak for large periods, related to site effect of soft soil: Mexican station at 2.5 sec., which caused the collapse of numerous buildings; and Ecuadorian station at 1.6 sec.

As stated before, bad seismic performance of most buildings was by many non-technical causes. Despite this reality, evident soil effect due to soft soils was observed in Chone station. Free soil vibration phenomenon confirms the observations which explain the collapse of some structures of low and medium height for this city. However, the damage could be more catastrophic if the natural period of tall buildings coincided with the soil deposit period of 1.6 sec., as occurred in Mexico City, 1985. This represents a warning voice for the future development of high-rise building projects in Chone and other cities settled over soft soils in Ecuador.

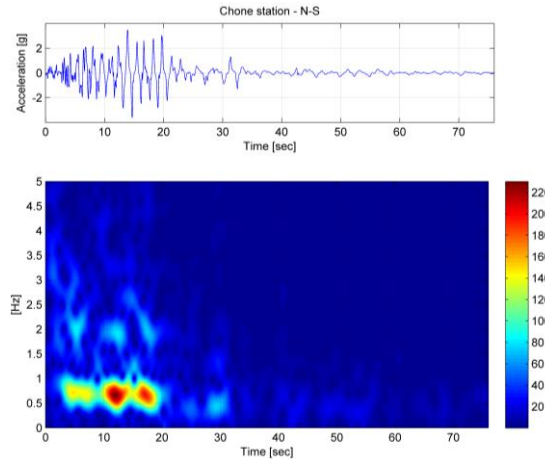


Fig. 6 – Spectrogram for Chone station (NS component). 2016 Muisne, Ecuador earthquake.

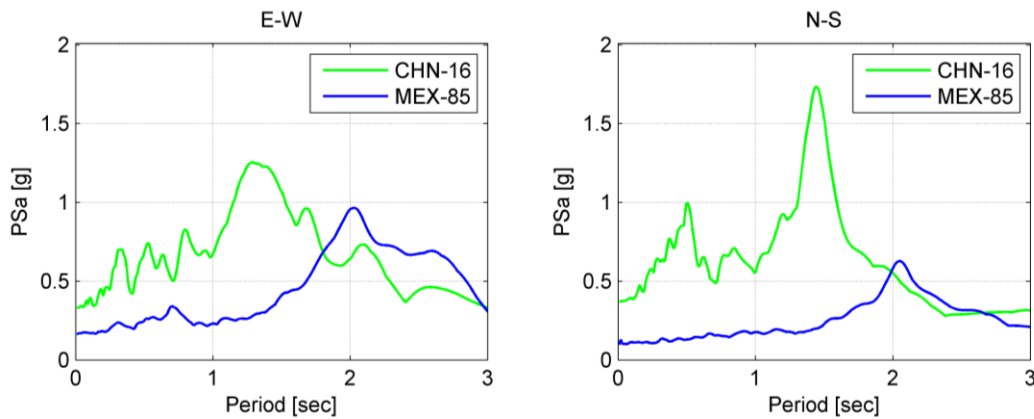


Fig. 7 – Acceleration response spectra for American interplate subduction earthquakes,  $\beta=5\%$ . Green: Chone station, 2016. Blue: SCT, Mexico City station, 1985.

## 7. H/V Spectral Ratio

The horizontal-to-vertical spectral ratio  $R_{H/V}$ , defined by Nakamura [24], is the ratio between horizontal and vertical surface components of microtremor records in the frequency domain, measured on ground level. Nakamura assumes that the H/V ratio, defined according Eq. (4), corresponds to the transfer function of the surface levels subjected to horizontal movements.  $S_{HS}$  and  $S_{VS}$  represent the Fourier amplitude spectra of the horizontal and vertical motions at the surface of a soil deposit, respectively.

$$R_{H/V} = \frac{S_{HS}}{S_{VS}} \quad (4)$$

As it is performed for microtremor vibrations, this method can be applied to calculate the H/V spectral ratio between horizontal and vertical components recorded at the surface, considering temporary windows of the accelerograph record. Lermo and Chavez-García [25] applied this method for some Mexican seismic records, obtaining fundamental frequencies of soil deposits which agreed with those obtained by the standard spectral ratio method. For Pedernales and Chone stations, H/V spectral ratio were determined considering the coda of the horizontal and vertical accelerograms. This part of the record contains the surface waves and the free vibration of the soil deposit after the earthquake. For Pedernales station, the window length is 30 sec., from 40 to 70 sec. while for Chone station the window length is also 30 sec., from 50 to 80 sec. Fig. 8 shows the predominant period of the soil deposit of 0.5 sec. ( $f = 2.0$  Hz) and 1.6 sec. ( $f = 0.6$  Hz) for Pedernales and Chone, respectively. The values of predominant periods determined for these two cities have a good correlation with values obtained from the second peak of the acceleration spectra due to soil response shown in Fig. 5 and Fig. 7.

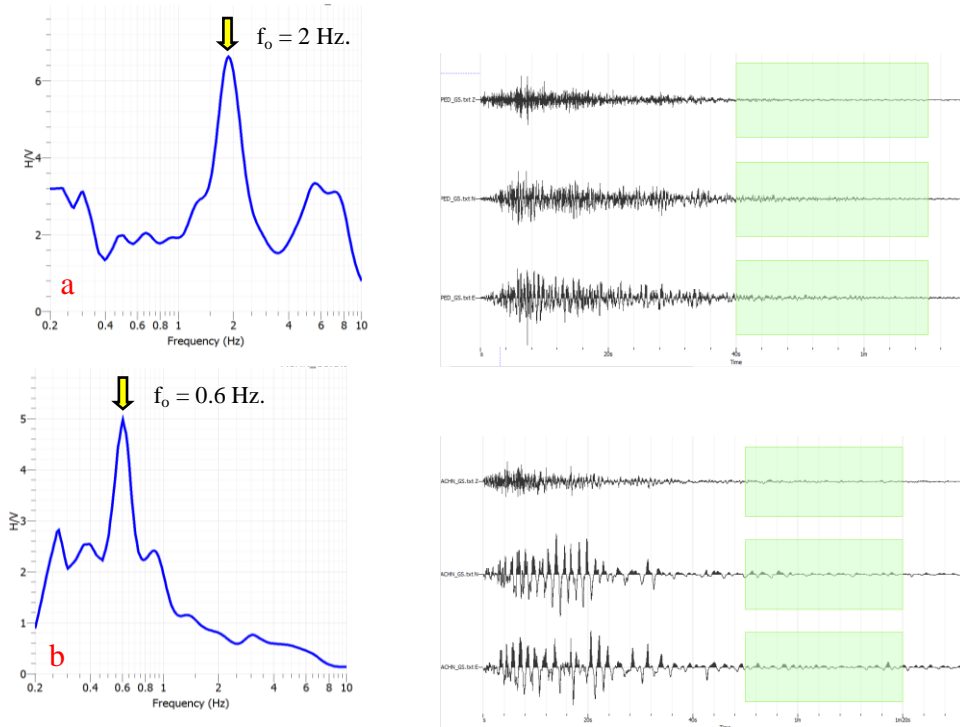


Fig. 8 – H/V spectral ratio obtained from the accelerogram codas for 2016 Muisne, Ecuador earthquake. a) Pedernales station. b) Chone station.

## 8. Conclusions

Due to the geographic location, Ecuador presents seismological characteristics typical of major zones related to energy liberation, like the west coast of the United States or the Chilean coast, showing its important incidence in the world seismic history from earthquakes such as Esmeraldas 1906. The event of April 2016 confirms the concept of the seismic gap offshore the Atacames promontory, completing the seismic cycle that began in 1906.

The analysis of 21 seismic records of the RENAC stations shows that phenomena like attenuation, directivity and amplification, which are typical of subduction seismic events in Chile and Peru with elongated elliptic shape of the shaken area in a direction parallel to the coastline, is also observed in the Muisne earthquake. The Andean Mountains act as a natural barrier, providing greater seismic attenuation in the EW direction

The instrumental analysis of high values of PGA (1.41 g., Pedernales station) and Pdh (583.5 cm-sec., Chone station) confirms the observations indicating that the Muisne event was destructive. Six stations of 21 have destructive accelerograms, which correspond to cities where damaging conditions and building collapses were observed. Despite Guayaquil station has the lowest Pdh value, EMS-98 intensity of VI was reported for the city. This fact is due to the station is located over superficial rock, while downtown is settled over soft silt/sandy soils.

Pedernales, the nearest station to the epicenter, is characterized to have their response spectra with two predominant peaks. One of them around 0.5 sec., which would belong to the free vibrations of the soft soil; and another peak around 0.1 sec., due to probably the interaction of the waves associated with the seismic source.

For Pedernales and Chone stations, H/V spectral ratio were determined considering the coda of the accelerograms, obtaining predominant periods of the soil deposit of 0.5 and 1.6 sec., respectively. This periods have a good correlation with those obtained from the second peak of the response spectra due to soil response.

Soil effects could be inferred due to the high destructiveness potential, the low zero crossing intensity and free soil vibration phenomenon in some accelerograms. All these remarks evidence the high seismic hazard in Ecuador and represents a warning voice for the future development of high-rise building projects in many cities settled over soft soils along the country.



## 9. References

- [1] CNDM - IRD - INOCAR (2009): Geología y Geofísica Marina y Terrestre del Ecuador PSE-001-2009, 278p.
- [2] USGS (2016): Largest Earthquakes in the World Since 1900. <http://earthquake.usgs.gov/earthquakes/world/>
- [3] Rudolph E, Szirtes S (1911): Das Kolumbianische Erdbeben Am 31 Januar 1906. *Gerlands Beiträge zur Geophysik*, Leipzig, Germany.
- [4] Engdahl ER, Villaseñor A (2002): Global Seismicity: 1900-1999. *International Handbook of Earthquake and Engineering Seismology, Part A*, 43, 665-690.
- [5] Kelleher J (1972): Rupture zones of large South American earthquakes and some predictions. *Journal of Geophysical Research Atmospheres*. Res. 77, 2087-2103
- [6] Kanamori H, McNally KC (1982): Variable rupture mode of the subduction zone along the Ecuador–Colombia coast. *Bulletin of the Seismological Society of America*. 72 (4), 1241–1253.
- [7] Swenson JL, Beck SL (1996): Historical 1942 Ecuador and 1942 Peru subduction earthquakes, and earthquake cycles along Colombia–Ecuador and Peru subduction segments. *Pure Appl. Geophys*. 146 (1), 67–101.
- [8] Collot JY, Agudelo W, Ribodetti A, (2008): Origin of a crustal splay fault and its relation to the seismogenic zone and underplating at the erosional north Ecuador–south Colombia oceanic margin. *J. Geophys. Res*. 113.
- [9] Nocquet JM., Villegas-Lanza JC, Chlieh M, Mothes PA, Yepes H (2014): Motion of continental slivers and creeping subduction in the northern Andes. *Nat. Geosci*. 7 (4), 287–291.
- [10] Chlieh M, Mothes PA, Nocquet JM, Yepes H (2014): Distribution of discrete seismic asperities and aseismic slip along the Ecuadorian megathrust. *Earth and Planetary Science Letters*. 400, 292–301.
- [11] USGS (2016): M 7.8 - 27km SSE of Muisne, Ecuador. <http://earthquake.usgs.gov/earthquakes/eventpage/us20005j32>
- [12] IASPEI (2002): *International Handbook of Earthquake and Engineering Seismology, Part A*.
- [13] Singaicho JC, Laurendeau A, Viracucha C, Ruiz M (2016): Observaciones del sismo del 16 de Abril de 2016 de magnitud Mw 7.8, Intensidades y Aceleraciones. *Sometido a la Revista Politécnica*.
- [14] IG-EPN (2016): Sismo Mw=7.8; 16 abril de 2016. <http://www.igepn.edu.ec/mapas/mapa-evento-20160416.html>
- [15] EERI (2016): M7.8 Muisne, Ecuador Earthquake on April 16, 2016. *EERI Earthquake Reconnaissance Team Report*.
- [16] Saragoni GR, Ruiz S (2012): Capítulo 6 - Implicaciones y nuevos desafíos de diseño sísmico de los acelerogramas del terremoto del 2010. Mw=8,8: *Terremoto en Chile, 27 de febrero de 2010*. Departamento de Ingeniería Civil, Santiago.
- [17] Arias A (1970): A measure of earthquake intensity. *Seminar on Seismic Design for Nuclear Power Plant*. Massachusetts Institute of Technology, Cambridge, Massachusetts, USA.
- [18] Araya R, Saragoni GR (1980): Capacity of seismic motion to produce structural damage. *SES I 7/80*. Departamento de Ingeniería Civil, Universidad de Chile, Santiago.
- [19] Saragoni GR, Holmberg A, Saez A. (1989): Destructiveness potential and the destructiveness of the 1985 Chile earthquake. *5th Chilean Conference of Seismology and Earthquake Engineering*, Santiago, Chile. vol. 1, pp. 369-378.
- [20] Saragoni GR, Astroza M, Ruiz S (2008): Study of the Accelerogram Destructiveness of Nazca Plate Subduction Earthquakes. *The 14th World Conference on Earthquake Engineering*, Beijing, China.
- [21] Saragoni GR, Herrera O (1993): Estudio comparativo de la Capacidad Destructiva de los Terremotos de Chile y Mexico de 1985. *5tas Jornadas chilenas de Sismología e Ingeniería Antisísmica*, Santiago, Chile, Vol II, 179-190.
- [22] Laurendeau A, Ruiz M, Singaicho JC (2016): Observaciones del Sismo de 16 de abril de 2016 (Mw7.8) en la Ciudad de Guayaquil. *Informe Sísmico Especial N.-19*.
- [23] Ruiz S, Saragoni GR (2009): Free Vibration of Soils During Large Earthquakes. *Soil Dynamic and Earthquake Engineering*. 29, 1-16.
- [24] Nakamura Y (1989): A method for dynamic characteristics estimation of subsurface using microtremor on the ground surface. *Quarterly Reports of the Railway Technical Research Institute*, 30, 25–33.
- [25] Lermo J, Chavez-García FJ (1993): Site effect evaluation using spectral ratios with only one station. *Bull. Seism. Soc. Am.*, 83, 1574-1594.